World Academy of Science, Engineering and Technology
International Journal of Mathematical and Computational Sciences
Vol:8, No:2, 2014

Obstacle and Collision Avoidance Control Laws of a Swarm of Boids

Bibhya Sharma, Jito Vanualailai, Jai Raj

Open Science Index, Mathematical and Computational Sciences Vol:8, No:2, 2014 publications.waset.org/9997323/pdf

Abstract—This paper proposes a new obstacle and collision avoidance control laws for a three-dimensional swarm of boids. The swarm exhibit collective emergent behaviors whilst avoiding the obstacles in the workspace. While flocking, animals group up in order to do various tasks and even a greater chance of evading predators. A generalized algorithms for attraction to the centroid, inter-individual swarm avoidance and obstacle avoidance is designed in this paper. We present a set of new continuous time-invariant velocity control laws is presented which is formulated via the Lyapunov-based control scheme. The control laws proposed in this paper also ensures practical stability of the system. The effectiveness of the proposed control laws is demonstrated via computer simulations.

Keywords—Lyapunov-based Control Scheme, Motion planning, Practical stability, Swarm.

I. Introduction

A platform of biologically inspired concepts and behaviors has been applied into the real life situations. This has inspired researchers since numerous problems can be solved without rigorous mathematical approaches. It is basically the category of algorithms that imitate the way nature performs. This set of algorithms falls under various categories such as Artificial neural networks, Genetic algorithms, Evolutionary algorithms, Particle swarm optimization, Ant colony optimization, Fuzzy logic and others [1].

These have mostly prevailed in the field of robotics where solutions are sought for dull, dirty, difficult or dangerous tasks. The swarm behavior and its principles are now being used by scientists and researchers in many new approaches such as in optimization and in control of robots [2], [3]. The use of robots with the concept of swarming is significantly increasing in the manufacturing arena, not only for productivity enhancement but also for greater versatility and flexibility [4].

There is also the issue of limited resources which has brought about the use of multiple agents instead of single individuals. The advantages include flight control, satellite clustering, exploration, surveillance, foraging and cooperate manipulation [5], [6]. The applications of foraging could involve search-and-rescue teams at disaster sites. Teams of robots could be deployed to collect hazardous materials after a spill, nuclear reaction or other accidents in minimal time, hence, saving further loss in the environment. All in all, team(s) of homogeneous (even heterogeneous) robots working towards a common objective can satisfy stringent time, manpower and monetary demands, enhance performance and robustness, and harness desired multi-behaviors, each of which is extremely difficult if not entirely impossible to obtain from single agents [7].

The artificial potential field method has been frequently utilized to solve a wide range of problems permeating from robotic applications. Algorithms in this category tend to use physical analogies to establish artificial potential fields with repulsive fields around obstacles and attractive fields around goals [8]. A collision free path is determined by how much the robot is attracted to or repelled by the poles. The governing principle behind the artificial potential field method is to attach attractive field to the target and a repulsive field to each of the obstacles. Artificial potential fields methods have several advantages, the most important one being the easier implementation. The other advantages includes easier analytic representation of system singularities, limitations, and inequalities, its simplicity, favorable processing speeds, decentralization and scalability features that outweighs other methods [9].

This paper considers the motion planning and control of the swarm model when obstacles are introduced into the workspace. That is, we construct a Lyapunov-like function via the LbCS that guarantees the emergent behavior arising from the swarm, considering all practical limitations and constraints due to fixed obstacles.

II. A Three-Dimensional Swarm Model and its Practical Stability

At time $t \geq 0$, let $(x_i(t), y_i(t), z_i(t))$, $i = 1, 2, \ldots, n$, be the planar position of the ith individual, which we shall define as a point mass residing in a disk of radius $r_i > 0$,

$$b_i = \left[(\mathbf{z}_1, \mathbf{z}_2, \mathbf{z}_3) \in \mathbb{R}^3 : (\mathbf{z}_1 - x_i)^2 + (\mathbf{z}_2 - y_i)^2 + (\mathbf{z}_3 - z_i)^2 \leq r_i^2\right].$$

Using the above notations, we have a system of first-order ODEs for the ith individual, assuming the initial condition at $t = t_0 \geq 0$:

$$\left.\begin{aligned} x_i'(t) &= v_i(t) \\ y_i'(t) &= w_i(t) \\ z_i'(t) &= u_i(t) \\ x_{i0} := x_i(t_0), y_{i0} &:= y_i(t_0), z_{i0} := z_i(t_0). \end{aligned}\right\} \quad (1)$$

Bibhya Sharma is with the School of Computing, Information & Mathematical Sciences, University of the South Pacific, Suva, Fiji (e-mail: sharma_b@usp.ac.fj).

Jito Vanualailai and Jai Raj are also with the School of Computing, Information & Mathematical Sciences, University of the South Pacific.

Open Science Index, Mathematical and Computational Sciences Vol:8, No:2, 2014 publications.waset.org/9997323/pdf

If $\mathbf{g}_i(\mathbf{x}) := (v_i, w_i, u_i) \in \mathbf{R}^3$ and $\mathbf{G}(\mathbf{x}) := (\mathbf{g}_1(\mathbf{x}), \ldots, \mathbf{g}_n(\mathbf{x})) \in \mathbb{R}^{3n}$, then our swarm system of n individuals is

$$\dot{\mathbf{x}} = \mathbf{G}(\mathbf{x}), \quad \mathbf{x}_0 = \mathbf{x}(t_0). \tag{2}$$

Definition 1: System (2) is said to be

(S1) practically stable if given (λ, A) with $0 < \lambda < A$, we have $\|\mathbf{x}_0 - \mathbf{x}^*\| < \lambda$ implies that $\|\mathbf{x}(t) - \mathbf{x}^*\| < A$, $t \geq t_0$ for some $t_0 \in \mathbb{R}_+$;

(S2) uniformly practically stable if *(S1)* holds for every $t_0 \in \mathbb{R}_+$.

The following comparison principle is adapted from [10] to analyse the practical stability of system (2),

$K = \{a \in C[\mathbb{R}_+, \mathbb{R}_+] : a(d)$ is strictly increasing in d and $a(d) \to \infty$ as $d \to \infty\}$,

$S(\rho) = \{\mathbf{x} \in \mathbb{R}^{3n} : \|\mathbf{x} - \mathbf{x}^*\| < \rho\}$ and, for any Lyapunov-like function $V \in C[\mathbb{R}_+ \times \mathbb{R}^{3n}, \mathbb{R}_+]$,

$$D^+V(t,x) := \limsup_{h \to 0^+} \begin{pmatrix} \frac{V(t+h, x+h\mathbf{G}(x))}{h} \\ \\ -\frac{V(t,x)}{h} \end{pmatrix}$$

for $(t, \mathbf{x}) \in \mathbb{R}_+ \times \mathbb{R}^{3n}$, noting that if $V \in C^1[\mathbb{R}_+ \times \mathbb{R}^{3n}, \mathbb{R}_+]$, then $D^+V(t, \mathbf{x}) = V'(t, \mathbf{x})$, where

$$V'(t, \mathbf{x}) = V_t(t, \mathbf{x}) + V_x(t, \mathbf{x})\mathbf{G}(\mathbf{x}).$$

Theorem 1: Lakshmikantham, Leela and Martynyuk [10]. Assume that

1. λ and A are given such that $0 < \lambda < A$;
2. $V \in C[\mathbb{R}_+ \times \mathbb{R}^{3n}, \mathbb{R}_+]$ and $V(t, \mathbf{x})$ is locally Lipschitzian in $\mathbf{x}$;
3. for $(t, \mathbf{x}) \in \mathbb{R}_+ \times S(A)$, $b_1(\|\mathbf{x} - \mathbf{x}^*\|) \leq V(t, \mathbf{x}) \leq b_2(\|\mathbf{x} - \mathbf{x}^*\|)$, $b_1, b_2 \in K$ and $D^+V(t, \mathbf{x}) \leq q(t, V(t, \mathbf{x}))$, $q \in C[\mathbb{R}^3_+, \mathbb{R}]$;
4. $b_2(\lambda) < b_1(A)$ holds.

Then the practical stability properties of the scalar differential equation

$$h'(t) = q(t, h), \quad h(t_0) = h_0 \geq 0,$$

imply the corresponding practical stability properties of system (2).

III. Deployment of Lyapunov-based Control Scheme

The principal objective is to construct an artificial potential field function (APF), that is, a Lyapunov-like function for motion planning and control of the swarm of n boids. From the Lyapunov-like function, we derive the velocity controls, v_i, w_i,and u_i, such that the swarm of boids will be able to exhibit swarming behavior in certain direction whilst avoiding collisions and obstacles. The control scheme appropriately combines these positive and negative potential functions to form a Lyapunov-like function candidate – a platform to design the nonlinear velocity controllers for the swarm of boids. This Lyapunov-like function candidate will also be utilized in a later section to prove the practical stability of the system.

A dichotomy of APFs will be designed in the following subsections, that is, we construct attractive functions and obstacle avoidance functions for the attraction to the centroid and the repulsion from the various obstacles, respectively.

A. Attraction to the Centroid

To ensure that the individuals of the swarm are attracted towards each other and also form a cohesive group by having a measurement of the distance from the ith individual to the swarm centroid, we use the following attraction function:

$$R_i(x) = \tfrac{1}{2}\left[\left(x_i - \tfrac{1}{n}\sum_{i=1}^{n} x_i\right)^2 + \left(y_i - \tfrac{1}{n}\sum_{i=1}^{n} y_i\right)^2 + \left(z_i - \tfrac{1}{n}\sum_{i=1}^{n} z_i\right)^2\right]$$

for $i \in \mathbb{N}$.

This will be part of a Lyapunov-like function for system (2) which ensures that ith individual is attracted to the swarm centroid.

B. Inter-individual Collision Avoidance

With system (1) of the ith individual in mind and for the boids to avoid each other, we use the following repulsive function:

$$Q_{ij}(\mathbf{x}) := \frac{1}{2}\left[(x_i - x_j)^2 + (y_i - y_j)^2 + (z_i - z_j)^2 - (r_i + r_j)^2\right].$$

The function is an Euclidean measure of the distance between the individual boids, and will appear in the denominator of an appropriate term in the candidate Lyapunov-like function.

C. Obstacle Avoidance

If a swarm encountered an obstacle in its path, how would it behave? Nature provides instances of the resultant behaviors – a flock of bird may split and then rejoin [11]; a swarm of zooplankton *Daphnia magna* may swirl about a marker [12], [13]; a bacterial swarm may increase its density in the presence of antibiotics [14], to name a few.

We now inject a set of solid objects fixed within the boundaries of the workspace and define an *obstacle space* for the stationary solid object. Since these objects can be of any shape (regular or irregular), we adopt the methodology given in [15], whereby the solid objects have been represented as simpler fixed-shaped objects such as a circle, a polygon or a convex hull [8], [5], to ensure that the entire body of an object is entirely within its obstacle space.

It can be verified geometrically that the most simplest fixed-shaped object in the Euclidean plane is a disk [8]. It is also a convenient form to use if we are using the Lyapunov-based Control Scheme to design controls [8]. Hence, we shall consider *disk-shaped* in a three-dimensional environment, simply *spherical-shaped obstacles*.

Other types of obstacles include *rod-shaped obstacles*, *elliptic-shaped obstacles* and moving obstacles such as *blindman* [8]. In this paper, we shall confine ourselves to spherical-shaped obstacles only to illustrates the effectiveness of the velocity controllers.

Let there be $m \in \mathbb{N}$ fixed obstacles within the boudary of the workspace. We have the following definition:

Open Science Index, Mathematical and Computational Sciences Vol:8, No:2, 2014 publications.waset.org/9997323/pdf

Definition 2: The kth spherical-shaped obstacle is centered at (o_{k1}, o_{k2}, o_{k3}), $k = 1, \cdots, m$, with radii $r_{ok} > 0$. Precisely, the kth disk-shaped obstacle is the set

$$\begin{aligned} o_k &:= \left\{(\mathbf{z}_1, \mathbf{z}_2, , \mathbf{z}_3) \in \mathbb{R}^3 : (\mathbf{z}_1 - o_{k1})^2 \right. \\ &\quad \left. +(\mathbf{z}_2 - o_{k2})^2 + (\mathbf{z}_3 - o_{k3})^2 \leq r_{ok}^2 \right\}. \end{aligned}$$

For the avoidance of these fixed obstacles, we consider the following obstacle avoidance function:

$$\begin{aligned} W_{ik}(\mathbf{x}) &:= \frac{1}{2}\Big[(x_i - o_{k1})^2 + (y_i - o_{k2})^2 \\ &\quad + (z_i - o_{k3})^2 - (r_i + r_{ok})^2\Big], \end{aligned}$$

for $i = 1, \cdots, n$ and $k = 1, \cdots, m$. The function $W_{ik}(\mathbf{x})$ is a measurement of the distance between the ith boid and kth obstacle o_k.

IV. Design of the Velocity Controllers

The nonlinear control laws for system (1) will be designed using the LbCS. In parallel, the control scheme will utilize Theorem 1 to provide the mathematical proof of the practical stability pertaining to system (1).

A. Lyapunov-like Function

AS per the LbCS, we combine all the attractive and the repulsive potential field functions designed in the previous sections and introduce *tuning parameters (or control parameters)* . With tuning parameter $\gamma_i > 0$, $\beta_{ij} > 0$ and $\omega_{ik} > 0$ $i, j, k \in \mathbb{N}$, we define a Lyapunov-like function for system (1) as

$$\begin{aligned} V_i(\mathbf{x}) &= L_i + \sum_{k=1}^{m} \frac{\omega_{ik} R_i(\mathbf{x})}{W_{ik}(\mathbf{x})} \\ &= \gamma_i R_i(\mathbf{x}) + \sum_{\substack{j=1,\\ j\neq i}}^{n} \frac{\beta_{ij} R_i(\mathbf{x})}{Q_{ij}(\mathbf{x})} + \sum_{k=1}^{m} \frac{\omega_{ik} R_i(\mathbf{x})}{W_{ik}(\mathbf{x})}, \end{aligned}$$

so that our new Lyapunov-like function for system (2) becomes

$$V(\mathbf{x}) := \sum_{i=1}^{n} V_i(\mathbf{x}_i),$$

which is clearly continuous and locally positive definite on the domain

$$E(V) := \mathbf{x} \in \mathbb{R}^{2n} : \sum_{i=1}^{n} \sum_{\substack{j=1,\\ j\neq i}}^{n} Q_{ij}(\mathbf{x}) > 0$$

and

$$\sum_{i=1}^{n} \sum_{k=1}^{m} W_{ik}(\mathbf{x}) > 0,$$

noting that $\mathbf{x}^* \notin E(V)$.

Assume next that the ratios are added appropriately to the Lyapunov-like function. Then any increase in a ratio *cannot* be unbounded because the existence of the Lyapunov-like function over an appropriate domain implies the boundedness of the state trajectories over the domain corresponding to any bounded initial condition within the domain. This means that the artificial potential field generated by $V(\mathbf{x})$ will not allow the swarms to get too close or collide with the obstacles. Note that any increase in the above ratios does not translate to an increase in $V \equiv V(t)$, simply because V, by its nature, is non-increasing in time $t \geq 0$ and any increase in one of the ratios gives a smaller or the same value of V at time t compared to all previous values of V.

As such, the essence of obstacle avoidance capability in the LbCS lies, therefore, in the creation of obstacle avoidance functions that will induce an increase or decrease in the instantaneous rate of change of the tentative Lyapunov-like function. The reader is referred to [8] for a detailed account of the effects of the obstacle avoidance functions and the resulting repulsive potential field functions.

B. Nonlinear Velocity Controllers

The time-derivative of V along every solution of system (2) is the dot product of the gradient of V, given by,

$$\nabla V = \left(\frac{\partial V}{\partial x_1}, \frac{\partial V}{\partial y_1}, \frac{\partial V}{\partial z_1}, \cdots, \frac{\partial V}{\partial x_n}, \frac{\partial V}{\partial y_n}, \frac{\partial V}{\partial z_n}\right),$$

and the time-derivative of the state vector $\mathbf{x} = (x_1, y_1, z_1, \ldots, x_n, y_n, z_n)$. That is,

$$\begin{aligned} \dot{V}(\mathbf{x}) &= \nabla V(\mathbf{x}) \bullet \dot{\mathbf{x}} \\ &= \sum_{i=1}^{n} \Bigg(\gamma_i \dot{R}_i(\mathbf{x}) + \sum_{\substack{j=1,\\ j\neq i}}^{n} \frac{\beta_{ij}}{Q_{ij}(\mathbf{x})} \dot{R}_i(\mathbf{x}) \\ &\quad - \sum_{\substack{j=1,\\ j\neq i}}^{n} \frac{\beta_{ij} R_i(\mathbf{x})}{Q_{ij}^2(\mathbf{x})} \dot{Q}_{ij}(\mathbf{x}) \\ &\quad + \sum_{k=1}^{m} \frac{\omega_{ik}}{W_{ik}(\mathbf{x})} \dot{R}_i(\mathbf{x}) \\ &\quad - \sum_{k=1}^{m} \frac{\omega_{ik} R_i(\mathbf{x})}{W_{ik}^2(\mathbf{x})} \dot{W}_{ik}(\mathbf{x}) \Bigg). \end{aligned}$$

Let there be real numbers $\mu_i > 0$, $\nu_i > 0$ and $\eta_i > 0$ such that

$$v_i = -\mu_i \frac{\partial V}{\partial x_i},\ w_i = -\nu_i \frac{\partial V}{\partial y_i} \quad \text{and} \quad u_i = -\eta_i \frac{\partial V}{\partial z_i}.$$

For the ith individual, system (1) therefore becomes

$$\begin{aligned} x_i'(t) &= v_i(t) = v_i(\mathbf{x}(t)) = -\mu_i \frac{\partial V}{\partial x_i}, \\ y_i'(t) &= w_i(t) = w_i(\mathbf{x}(t)) = -\nu_i \frac{\partial V}{\partial y_i}, \\ z_i'(t) &= u_i(t) = u_i(\mathbf{x}(t)) = -\eta_i \frac{\partial V}{\partial z_i}, \end{aligned} \tag{3}$$

$$x_{i0} = x_i(t_0), y_{i0} = y_i(t_0), z_{i0} = z_i(t_0), \ \ t_0 \geq 0,$$

Open Science Index, Mathematical and Computational Sciences Vol:8, No:2, 2014 publications.waset.org/9997323/pdf

where

$$\frac{\partial V}{\partial x_i} = \left(\gamma_i + \sum_{\substack{j=1,\\ j\neq i}}^{n} \frac{\beta_{ij}}{Q_{ij}(\mathbf{x})}\right)\left(x_i - \frac{1}{n}\sum_{k=1}^{n} x_k\right) - 2\sum_{\substack{j=1,\\ j\neq i}}^{n} \frac{\beta_{ij}R_i(\mathbf{x})}{Q_{ij}^2(\mathbf{x})}(x_i - x_j) - \sum_{k=1}^{m} \frac{\omega_{ik}R_i(\mathbf{x})}{W_{ik}^2(\mathbf{x})}(x_i - o_{k1}),$$

and

$$\frac{\partial V}{\partial y_i} = \left(\gamma_i + \sum_{\substack{j=1,\\ j\neq i}}^{n} \frac{\beta_{ij}}{Q_{ij}(\mathbf{x})}\right)\left(y_i - \frac{1}{n}\sum_{k=1}^{n} y_k\right) - 2\sum_{\substack{j=1,\\ j\neq i}}^{n} \frac{\beta_{ij}R_i(\mathbf{x})}{Q_{ij}^2(\mathbf{x})}(y_i - y_j) - \sum_{k=1}^{m} \frac{\omega_{ik}R_i(\mathbf{x})}{W_{ik}^2(\mathbf{x})}(y_i - o_{k2}),$$

and

$$\frac{\partial V}{\partial z_i} = \left(\gamma_i + \sum_{\substack{j=1,\\ j\neq i}}^{n} \frac{\beta_{ij}}{Q_{ij}(\mathbf{x})}\right)\left(z_i - \frac{1}{n}\sum_{k=1}^{n} z_k\right) - 2\sum_{\substack{j=1,\\ j\neq i}}^{n} \frac{\beta_{ij}R_i(\mathbf{x})}{Q_{ij}^2(\mathbf{x})}(z_i - z_j) - \sum_{k=1}^{m} \frac{\omega_{ik}R_i(\mathbf{x})}{W_{ik}^2(\mathbf{x})}(z_i - o_{k3}).$$

Then system (2) becomes the new gradient system

$$\dot{\mathbf{x}} = \mathbf{G}(\mathbf{x}) = -H\ (\nabla V(\mathbf{x})), \quad \mathbf{x}_0 := \mathbf{x}(t_0),\ \ t_0 \geq 0, \tag{4}$$

It is clear that $\mathbf{G} \in C[E(V), \mathbb{R}^{3n}]$.

V. Practical Stability Analysis

We shall prove the practical stability of system (4) using the method by Lakshmikantham, Leela and Martynyuk [10].

Theorem 2: System (4) is uniformly practically stable.

Proof. Since

$$\dot{V}(\mathbf{x}(t)) \leq 0,$$

we have

$$0 \leq V(\mathbf{x}(t)) \leq V(\mathbf{x}(t_0))\ \ \forall\ \ t \geq t_0 \geq 0. \tag{5}$$

Accordingly, for comparative analysis, it is sufficient to consider the practical stability of the scalar differential equation

$$h'(t) = 0,\ \ h(t_0) =: h_0,\ \ t_0 \geq 0. \tag{6}$$

The solution is

$$h(t; t_0, h_0) = h_0,$$

so that relative to every point $h^* \in \mathbb{R}$, we have

$$h(t; t_0, h_0 - h^*) = h_0 - h^*,$$

so that for any given number $P_0 > 0$,

$$|h(t; t_0, h_0 - h^*)| \leq |h_0 - h^*| + P_0.$$

We shall next show that by applying Theorem 1, we can simultaneously derive the explicit form of $P_0 > 0$, with which it is easy to see that (S2) holds for equation (6) if

$$A = A(\lambda) := \lambda + P_0.$$

To apply Theorem 1, we restrict our domain to $D(L)$ over which we see that $V \in C[D(V), \mathbb{R}_+]$, and note that V is locally Lipschitzian in $D(V)$ since $dV/dt \leq 0$ in $D(V)$. Re-defining $S(\rho)$ as $S(\rho) = \{\mathbf{x} \in D(V) : \|\mathbf{x} - \mathbf{x}^*\| < \rho\}$, we get

$$S(A) = \{\mathbf{x} \in D(V) : \|\mathbf{x} - \mathbf{x}^*\| < \lambda + P_0\}.$$

Recalling that $\gamma_i > 0$, $i \in \mathbb{N}$, we let

$$\gamma_{\min} := \min_{i\in\mathbb{N}} \gamma_i \quad \text{and } \gamma_{\max} := \max_{i\in\mathbb{N}} \gamma_i.$$

Further, let

$$b_1(\|\mathbf{x} - \mathbf{x}^*\|) := \frac{1}{2}\gamma_{\min}\|\mathbf{x} - \mathbf{x}^*\|^2$$

and

$$b_2(\|\mathbf{x} - \mathbf{x}^*\|) := \frac{1}{2}\gamma_{\max}\left[\|\mathbf{x} - \mathbf{x}^*\| + V(\mathbf{x}_0)\right]^2,$$

noting that $b_1, b_2 \in K$. Then assuming $P_0 > 0$ we easily see that with (5) we have

$$b_1(\|\mathbf{x} - \mathbf{x}^*\|) \leq V(\mathbf{x}) \leq b_2(\|\mathbf{x} - \mathbf{x}^*\|) \quad \text{for} \quad \mathbf{x} \in S(A),$$

since

$$\sum_{i=1}^{n} R_i(\mathbf{x}) \quad = \quad \frac{1}{2}\|\mathbf{x} - \mathbf{x}^*\|^2.$$

Indeed, the inequality $b_2(\lambda) < b_1(A)$ yields

$$\frac{1}{2}\gamma_{\max}\left[\lambda + V(\mathbf{x}_0)\right]^2 < \frac{1}{2}\gamma_{\min}[\lambda + P_0]^2,$$

which holds if we choose

$$P_0 > \left[\left(\sqrt{\frac{\gamma_{\max}}{\gamma_{\min}}} - 1\right) + \sqrt{\frac{\gamma_{\max}}{\gamma_{\min}}}L(\mathbf{x}_0)\right].$$

Since $\gamma_{\max}/\gamma_{\min} \geq 1$ for any $\gamma_{\max}, \gamma_{\min} > 0$, and because of (5), it is clear that P_0 exists and $P_0 > 0$. Thus, with $q(t, z) \equiv 0$, we conclude the proof of Theorem 2.

VI. Computer Simulations

To show the effectiveness of the control scheme, computer simulations were done using "Mathematica Software" for the swarm model.

Open Science Index, Mathematical and Computational Sciences Vol:8, No:2, 2014 publications.waset.org/9997323/pdf

A. Scenario 1: A Spiral-Like Behavior

We consider a situation where the swarm converges to a cylindrical obstacle, avoiding it and exhibit a spiral-like behavior. This could be modeled as a flock of boids moving in a spiral-like cruise formation. We consider 20 individuals, each with a bin size 20, initially randomly placed into the workspace. There are 20 spherical obstacles of radius 100 placed on top of each other to derive a cylindrical-type of obstacle. Fig. 1 shows the swarm (in red) moving about a field of cylindrical-type obstacles.

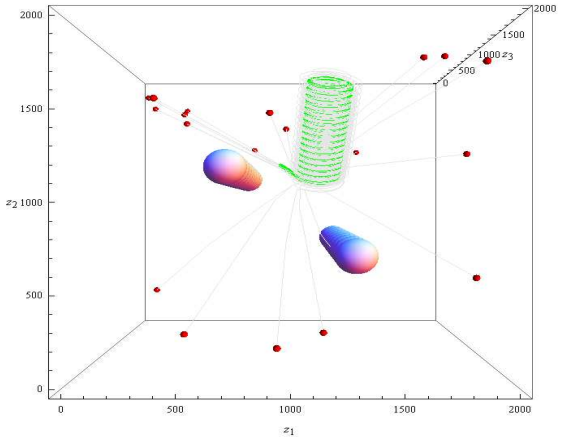
B. Scenario 2: A Spiral-Like Behavior

We consider a situation where the swarm converges and exhibit a spiral-like behavior. We consider 20 individuals, each with a bin size 20, initially randomly placed into the workspace. There are 50 spherical obstacles of radius 100 placed on top of each other to derive a cylindrical-type of obstacle. Fig. 2 shows the swarm (in red) moving about a field of cylindrical-type obstacles. The cohesion parameter plays a big role in inducing this particular emergent behavior in motion planning and control.

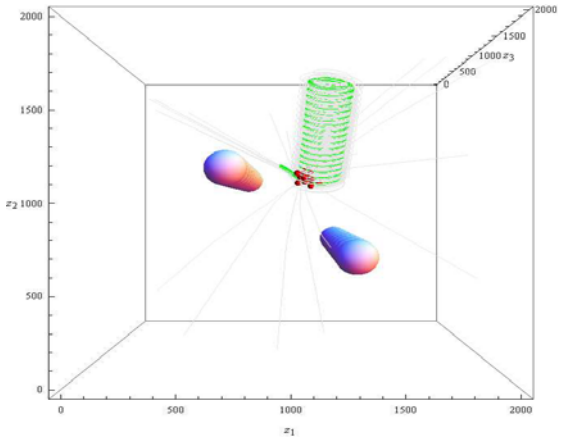
VII. Conclusion

Our proposed model is essentially a distributed control system wherein each individual has its own controller that controls its position and instantaneous velocities. In this paper, we have presented a set of distributed continuous time-invariant velocity control laws that results in the emergent swarm behaviors while avoiding obstacles and collisions in a constrained environment. The generalized controllers, extracted from the Lyapunov-based control scheme (LbCS), enabled collision free trajectories of the swarm within a constrained environment, whilst satisfying the intimately couple holonomic constraints of the swarm, and the kinodynamic constraints associated with the system. The effectiveness of the proposed control laws was demonstrated via computer simulations of different emerging behaviors.

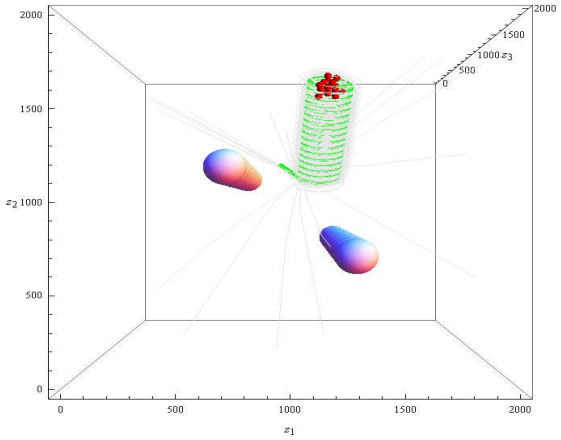
Future work will attempt to extend the results of this paper and focus on the behavior of a swarm with specific formations in tunnels.



(a) Initial state of the swarm ($t = 0$).



(b) State of the swarm at $t = 400$ units.



(c) State of the swarm at $t = 800$ units.

Fig. 1. The top view of the swarm whilst avoiding the cylindrical type obstacles. The parameters are α_i^s, $i = 1, \ldots, 20, s = 1, 2, 3$, randomized between 0.5 and 1, γ_i randomized between 0.5 and 1, $\beta_{ij} > 0$, $i, j \in \mathbb{N}$, $i \neq j$ randomized between 100 and 150 and $\omega_{ik} = 0.5$. The initial positions and the onset of swarming are shown in (a). In (b) and (c), the individuals (shown in red) congregate and group up and spiral past the obstacles. The trajectories are shown in grey. The centroid is shown by the green color.

References

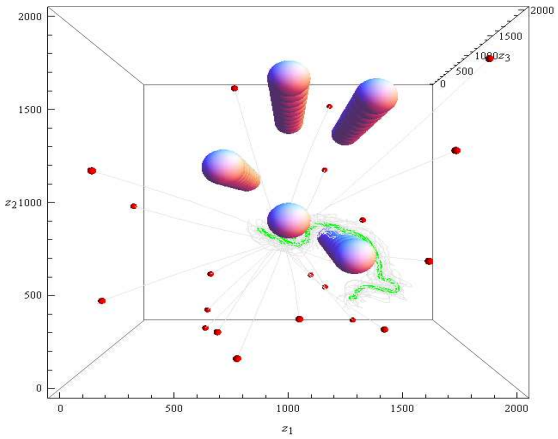
[1] C. Blum and D. Merkle. *Swarm Intelligence: Introduction and Applications*. Springer - Verlag Berlin Heidelberg, Germany, 2008.

[2] M. Dorigo, L.M. Gambardella, M. Birattari, A. Martinoli, R. Poli, and T. Stützle. *Ant Colony Optimization and Swarm Intelligence: 5th International Workshop, ANTS 2006, Brussels, Belgium, September 4-7, 2006, Proceedings*, volume 4150. Springer, 2006.

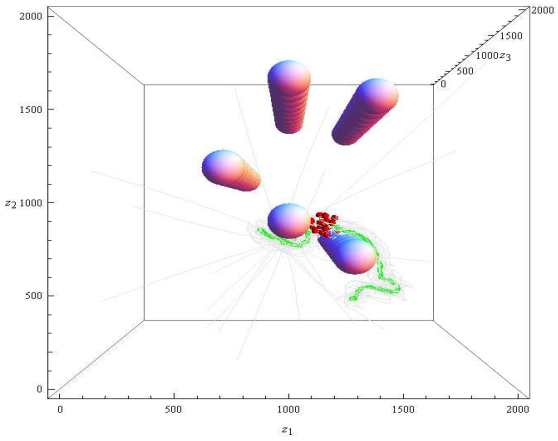
[3] Q.K. Pan, M. Fatih Tasgetiren, and Y.C. Liang. A discrete particle swarm optimization algorithm for the no-wait flowshop scheduling problem. *Computers & Operations Research*, 35(9):2807–2839, 2008.

[4] G.J. Gelderblom, G. Cremers, M. de Wilt, W. Kortekaas, A. Thielmann, K. Cuhls, A. Sachinopoulou, and I. Korhonen. The opinions expressed in this study are those of the authors and do not necessarily reflect the views of the european commission. 2008.

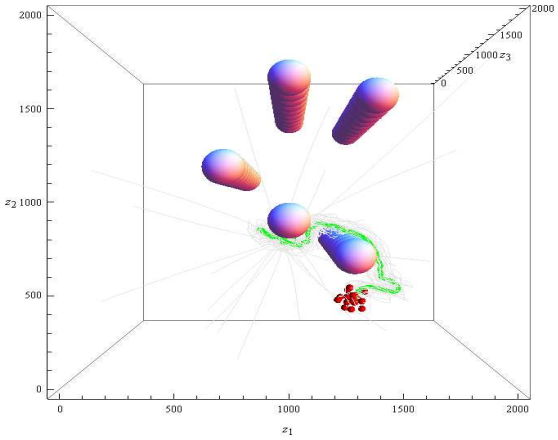
Open Science Index, Mathematical and Computational Sciences Vol:8, No:2, 2014 publications.waset.org/9997323/pdf



(a) Initial state of the swarm ($t = 0$).



(b) State of the swarm at $t = 400$ units.



(c) State of the swarm at $t = 100$ units.

Fig. 2. Compactness and mobility for obstacle avoidance. The parameters are α_i^s, $i = 1, \ldots, 20, s = 1, 2, 3$, randomized between 0.5 and 1, γ_i randomized between 0.5 and 1, $\beta_{ij} > 0$, $i, j \in \mathbb{N}$, $i \neq j$ randomized between 100 and 150 and $\omega_{ik} = 0.5$. The initial positions and the onset of swarming are shown in (a). In (b) and (c) the individuals (shown in red) congregate and group to swirl past the obstacle and settles into a cruise formation. The trajectories are shown in grey. The centroid is shown by the green color.

[5] B. Sharma, J. Vanualailai, and S. Singh. Tunnel passing maneuvers of prescribed formations. *International Journal of Robust and Nonlinear Control*, 2012.

[6] B. Sharma, J. Vanualailai, and S. Singh. Lyapunov-based nonlinear controllers for obstacle avoidance with a planar -link doubly nonholonomic manipulator. *Robotics and Autonomous Systems*, 2012.

[7] B. Sharma, J. Vanualailai, and U. Chand. Flocking of multi-agents in constrained environments. *European Journal of Pure and Applied Mathematics*, 2(3):401–425, 2009.

[8] B. Sharma. *New Directions in the Applications of the Lyapunov-based Control Scheme to the Findpath Problem*. PhD thesis, University of the South Pacific, Suva, Fiji Islands, July 2008. PhD Dissertation.

[9] O. Lefebvre, F. Lamiraux, and C. Pradalier. Obstacles avoidance for car-like robots: Integration and experimentation on two robots. In *IEEE International Conference on Robotics and Automation*, New Orleans, April 26th - May 1st 2004.

[10] V. Lakshmikantham, S. Leela, and A. A. Martynyuk. *Practical Stability of Nonlinear Systems*. World Scientific, Singapore, 1990.

[11] C. W. Reynolds. Flocks, herds, and schools: A distributed behavioral model, in computer graphics. In *Proceedings of the 14th annual conference on Computer graphics and interactive techniques*, pages 25–34, New York, USA, 1987.

[12] A. Ordemann, G. Balazsi, and F. Moss. Pattern formation and stochastic motion of the zooplankton *Daphina* in a light field. *Physica A*, 325:260–266, 2003.

[13] F. Moss. Into the *Daphina* vortex. *Chaos*, 14(4):S10, 2004.

[14] M. T. Butler, Q. Wang, and R. M Harshy. Cell density and mobility protect swarming bacteria against antibiotics. *Proceedings of the National Academy of Sciences*, 107(8):3776–3781, 2010.

[15] P. C-Y. Sheu and Q. Xue. *Intelligent Robotic Planning Systems*. World Scientific, Singapore, 1993.